



Digital Receipt

This receipt acknowledges that Turnitin received your paper. Below you will find the receipt information regarding your submission.

The first page of your submissions is displayed below.

Submission author: Jeffry Julianus
Assignment title: Periksa similarity
Submission title: Arylamide as potential selective inhibitor for matrix metallo...
File name: gn_synthesis_biological_evaluation_and_molecular_modelin...
File size: 4.16M
Page count: 11
Word count: 8,853
Character count: 45,248
Submission date: 20-Jul-2022 09:02AM (UTC+0700)
Submission ID: 1872830950

JCM JOURNAL OF CHEMICAL INFORMATION AND MODELING
Cite This: J. Chem. Inf. Model. 2020, 10, 349–359
pubs.acs.org/jcim

Arylamide as Potential Selective Inhibitor for Matrix Metalloproteinase 9 (MMP9): Design, Synthesis, Biological Evaluation, and Molecular Modeling

Maywan Hariono,¹ Rina F. Nugranda,² Muhammad Yusuf,³ Rollando Rollando,⁴ Riris I. Jenie,¹ Belal Al-Najar,⁵ Jeffry Julianus,⁶ Kevin C. Putra,⁷ Ervan S. Nugroho,⁸ Yohanes K. Wisnumurti,⁹ Sangga P. Deva,¹ Benedictus W. Jati,¹ Reynaldo Tiara,¹ Ratna D. Ramadani,¹ Lailatul Qodria,¹ and Habibah A. Wahab¹

¹Faculty of Pharmacy, Sanata Dharma University, Depok, Sleman 55282, Yogyakarta, Indonesia
²Faculty of Pharmacy, Padjadjaran University, Jatinangor, Sumedang 45363, West Java, Indonesia
³Chemistry Department, Faculty of Mathematics and Natural Sciences, Padjadjaran University, Jatinangor, Sumedang 45363, West Java, Indonesia
⁴Pharmacy Program, Faculty of Science and Technology, Ma Chung University, Malang 65151, Indonesia
⁵Cancer Chemoprevention Research Center, Faculty of Pharmacy, Gadjah Mada University, Sekip Utara 55281, Yogyakarta, Indonesia
⁶Faculty of Pharmacy and Medical Sciences, AlAbditya Amman University, Amman 19338, Jordan
⁷Pharmaceutical Technology Department, School of Pharmaceutical Sciences and USM-RIKEN Centre for Ageing Science (URICAS), Universiti Sains Malaysia, 11800 Minden, Pulau Pinang, Malaysia

Supporting Information

ABSTRACT: Previous studies have reported that compounds bearing an arylamide linked to a heterocyclic planar ring have successfully inhibited the hemopexin-like domain (PEXV) of matrix metalloproteinase-9 (MMP9). PEXV has been suggested to be more selectively targeted than MMP9's catalytic domain in a degrading extracellular matrix under some pathologic conditions, especially in cancer. In this study, we aim to synthesize and evaluate 10 arylamide compounds as MMP9 inhibitors through an enzymatic assay as well as a cellular assay. The mechanism of inhibition for the most active compounds was investigated via molecular dynamics simulation (MD). Molecular docking was performed using AutoDock4.0 with PEXV as the protein model to predict the binding of the designed compounds. The synthesis was carried out by reacting aniline derivatives with 3-hemopexinopropionyl chloride using pyridine as the catalyst at room temperature. The MMP9 assay was conducted using the FRET-based MMP9 kits protocol and gelatin zymography assay. The cytotoxicity assay was done using the MTT method, and the MD simulation was performed using AMBER16. Assay on MMP9 demonstrated activities of three compounds (2, 7, and 9) with more than 50% inhibition. Further inhibition on MMP9 expressed by 471 showed that two compounds (7 and 9) inhibited its gelatinolytic activity more than 50%. The cytotoxicity assay against 471 cells results in the inhibition of the cell growth with an EC_{50} of 125 μ M and 132 μ M for 7 and 9, respectively. The MD simulation explained a stable interaction of 7 and 9 in PEXV at 100 ns with a free energy of binding of -8.03 kcal/mol and -6.41 kcal/mol, respectively. Arylamides have potential effects as selective MMP9 inhibitors in inhibiting breast cancer cell progression.

INTRODUCTION

Breast cancer, the most common cancer in females, is now the second leading cause of death related to cancer in the world.¹ As with any other cancer, the disease is attributed to complicated pathways, in which cell selectivity becomes the major issue in its pharmacotherapy.² The development of anticancer chemotherapeutic agents by targeting selective proteins or nucleic acid for breast cancer is challenging and mostly met with some serious adverse side effects as well as resistance.³

Breast cancer is categorized into three types according to the most common receptors known to fuel breast cancer growth, i.e., estrogen, progesterone, and human epidermal growth factor receptor 2 (HER-2).⁴ Another type in which these three receptors are not present is called a triple-negative type.⁵ Several proteins have been reported to be responsible for cancer cell growth. However, in triple-negative breast cancer,

Received: July 30, 2019
Published: December 11, 2019

ACS Publications | © 2019 American Chemical Society | 349
DOI: 10.1021/acs.jcim.9b00355
J. Chem. Inf. Model. 2020, 10, 349–359

Arylamide as potential selective inhibitor for matrix metalloproteinase 9 (MMP9) design, synthesis, biological evaluation, and molecular modeling

by Julianus Jeffry

Submission date: 20-Jul-2022 09:02AM (UTC+0700)

Submission ID: 1872830950

File name: gn_synthesis_biological_evaluation_and_molecular_modeling.pdf (4.16M)

Word count: 8853

Character count: 45248

Arylamide as Potential Selective Inhibitor for Matrix Metalloproteinase 9 (MMP9): Design, Synthesis, Biological Evaluation, and Molecular Modeling

Maywan Hariono,^{*,†} Rina F. Nuwarda,[‡] Muhammad Yusuf,[§] Rollando Rollando,^{||} Riris I. Jenie,[⊥] Belal Al-Najjar,[#] Jeffry Julianus,[†] Kevin C. Putra,[†] Ervan S. Nugroho,[†] Yohanes K. Wisnumurti,[†] Sangga P. Dewa,[†] Benedictus W. Jati,[†] Reynaldo Tiara,[†] Ratna D. Ramadani,[⊥] Lailatul Qodria,[⊥] and Habibah A. Wahab[¶]

[†]Faculty of Pharmacy, Setiata Dharma University, Depok, Sleman 55282, Yogyakarta, Indonesia

[‡]Faculty of Pharmacy, Padjadjaran University, Jatinangor, Sumedang 45363, West Java, Indonesia

[§]Chemistry Department, Faculty of Mathematics and Natural Sciences, Padjadjaran University, Jatinangor, Sumedang 45363, West Java, Indonesia

^{||}Pharmacy Program, Faculty of Science and Technology, Ma Chung University, Malang 65151, Indonesia

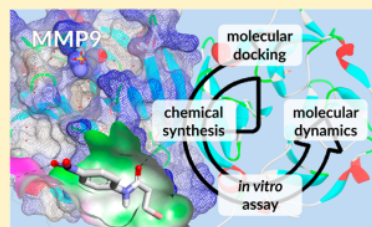
[⊥]Cancer Chemoprevention Research Center, Faculty of Pharmacy, Gadjah Mada University, Sekip Utara 55281, Yogyakarta, Indonesia

[#]Faculty of Pharmacy and Medical Sciences, AlAhliyya Amman University, Amman 19328, Jordan

[¶]Pharmaceutical Technology Department, School of Pharmaceutical Sciences and USM-RIKEN Centre for Ageing Science (URICAS), Universiti Sains Malaysia, 11800 Minden, Pulau Pinang, Malaysia

Supporting Information

ABSTRACT: Previous studies have reported that compounds bearing arylamide linked to a heterocyclic planar ring have successfully inhibited the hemopexin-like domain (PEX9) of matrix metalloproteinase 9 (MMP9). PEX9 has been suggested to be more selectively targeted than MMP9's catalytic domain in a degrading extracellular matrix under some pathologic conditions, especially in cancer. In this study, we aim to synthesize and evaluate 10 arylamide compounds as MMP9 inhibitors through an enzymatic assay as well as a cellular assay. The mechanism of inhibition for the most active compounds was investigated via molecular dynamics simulation (MD). Molecular docking was performed using AutoDock4.0 with PEX9 as the protein model to predict the binding of the designed compounds. The synthesis was carried out by reacting aniline derivatives with 3-bromopropanoyl chloride using pyridine as the catalyst at room temperature. The MMP9 assay was conducted using the FRET-based MMP9 kits protocol and gelatin zymography assay. The cytotoxicity assay was done using the MTT method, and the MD simulation was performed using AMBER16. Assay on MMP9 demonstrated activities of three compounds (2, 7, and 9) with more than 50% inhibition. Further inhibition on MMP9 expressed by 4T1 showed that two compounds (7 and 9) inhibited its gelatinolytic activity more than 50%. The cytotoxicity assay against 4T1 cells results in the inhibition of the cell growth with an EC₅₀ of 125 μ M and 132 μ M for 7 and 9, respectively. The MD simulation explained a stable interaction of 7 and 9 in PEX9 at 100 ns with a free energy of binding of -8.03 kcal/mol and -6.41 kcal/mol, respectively. Arylamides have potential effects as selective MMP9 inhibitors in inhibiting breast cancer cell progression.



20

INTRODUCTION

Breast cancer, the most common cancer in females, is now the second leading cause of death related to cancer in the world.¹ As with any other cancer, the disease is attributed to complicated pathways, in which cell selectivity becomes the major issue in its pharmacotherapy.² The development of anticancer chemotherapeutic agents by targeting selective proteins or nucleic acid for breast cancer is challenging and mostly met with some serious adverse side effects as well as resistance.³

Breast cancer is categorized into three types according to the most common receptors known to fuel breast cancer growth, i.e., estrogen, progesterone, and human epidermal growth factor receptor 2 (HER-2).⁴ Another type in which those three receptors are not present is called a triple-negative type.⁵ Several proteins have been reported to be responsible for cancer cell growth. However, in triple-negative breast cancer,

Received: July 30, 2019

Published: December 11, 2019

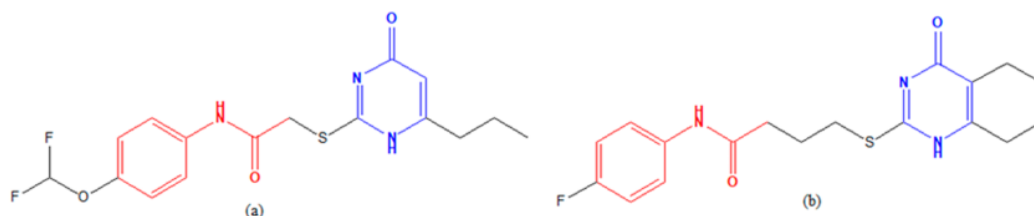
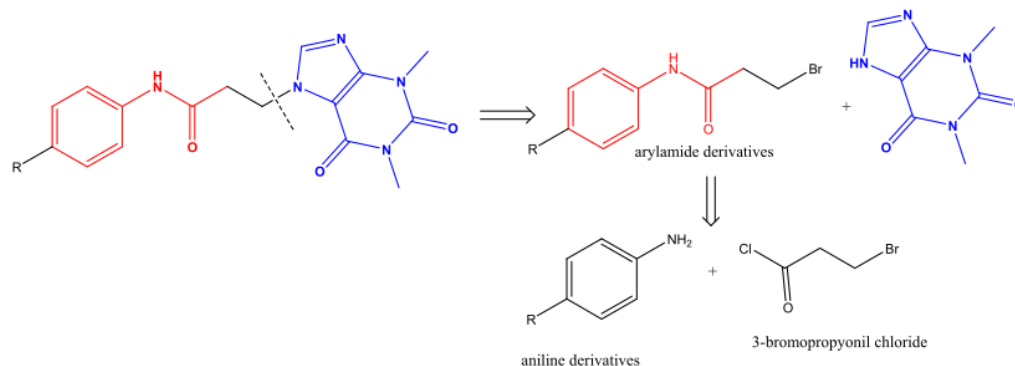


Figure 1. Structure and pharmacophore of active compound from (a) Dufour et al. ($K_d = 2.1 \mu\text{M}$)¹⁷ and (b) Alford et al. ($K_d = 320 \text{ nM}$)¹⁸ as a PEX9 inhibitor. The red and blue parts are the arylamide and heterocyclic planar ring, respectively.

Scheme 1. Retrosynthesis of a PEX9 Inhibitor Model to Yield Arylamide Derivatives and Purine As the Starting Materials⁴²



⁴²The red and blue parts are arylamide and heterocyclic planar ring, respectively. The arylamide itself is synthesized from aniline derivatives and 3-bromopropionyl chloride (acetyl chloride derivatives).

matrix metalloproteinase 9 (MMP9) has been identified to be highly expressed during angiogenesis as well as cell migration.⁶ MMP9 is one of the MMP subfamilies, classified as gelatinase that degrades the extracellular matrix (ECM). It also has 6 lamin as the substrate for the enzyme activity.^{7,8} The genomic structure of MMP9 is composed of the propeptide and a catalytic domain, which is bridged by SH-Zn, followed by three fibronectins, which are linked to the terminal hemopexin-like (PEX9) domain.^{9,10} The enzyme is activated by disconnecting the SH-Zn bridge (called a cysteine switch) to interact with the substrate.^{11,12} Therefore, by interrupting this interaction using peptidomimetics or small molecules, the progress of angiogenesis and cell migration could be well controlled.¹³ Unfortunately, many MMP9 inhibitors failed in the clinical trials due to the presence of adverse drug side effects (ADS) such as musculoskeletal syndrome.¹⁴ High homology in all MMP catalytic sites has been suggested to contribute to a nonselective inhibition leading to ADS.^{15,16}

Dufour et al. and Alford et al. have developed MMP9 inhibitors by targeting the noncatalytic site, i.e., hemopexin-like domain (PEX9).^{17,18} This domain has low-homology among all MMPs. Therefore, it is an interesting target for disrupting breast cancer with less adverse side effects.^{19,20} Dufour et al. studied the pharmacophore of two of their most active inhibitors (Figure 1a) via molecular docking into the binding site of PEX9. They suggested that the enzyme inhibitory activity, on one hand, was due to the six-member heterocycle ring, which provides a planar conformation that fits into the cavity of PEX9 domain blades. On the other hand, the arylamide moiety facilitates a flexible conformation that bound to the surface near the cavity.¹⁷

Analogues of these inhibitors could be synthesized by modifying the heterocyclic planar ring using purine, as suggested in Scheme 1. The retrosynthesis identified that the analogues could be synthesized through the nucleophilic acyl substitution reaction between the arylamide with bromine attached at the alkyl chain's terminus as the leaving group and purine. Thus, the arylamide has a role as an intermediate compound, which in turn could be synthesized from aniline derivatives with acetyl chloride derivatives.

In this present study, we designed and synthesized 10 arylamide compounds via modifications at its *para* position. The design was initiated by studying the binding mode of these compounds in the PEX9 binding site via molecular docking. The compounds were then evaluated for their potency to inhibit the activity of MMP9 using fluorescence binding and gelatin zymography assays. Then, the cytotoxicity assay was performed on the selected active compounds to the cell growth of 4T1, a cell model for the triple-negative breast cancer. Finally, a molecular dynamics study was carried out to gain a deep understanding of the interaction of the most active compounds with PEX9. This study found three compounds that are potentially developed as antibreast cancer agents.

METHODS

Molecular Design. The protein (PEX9, PDB ID 1ITV) was downloaded from www.rcsb.org.²¹ The control docking was carried out by extracting the sulfate ligand from PEX9 using Discovery Studio 3.5 (www.accelrys.com) and then prepared using AutodockTools 1.5.6 (www.scripps.edu).²² The protein was protonated and assigned Kollman charges, while the ligand was assigned Gasteiger charges. The grid box was set

with the number of grid points = $70 \times 70 \times 70$; grid point spacing = 0.375 Å; and the center of coordinates at $x = 42.053$, $y = -30.855$, and $z = -1.804$. Docking was performed using AutoDock 4.2 with the Lamarckian Genetic Algorithm (LGA) for 250 iterations. The free energy of binding was calculated as the sum of the final intermolecular energy, van der Waals, H-bond, desolvation, electrostatic, final total internal energy, torsional free, and unbound system energy. The docking poses were visualized using Discovery Studio 3.5, and the docking parameter was defined as valid when the RMSD value between initial and postdocking poses was not greater than 2.0 Å.²³ The new ligands were sketched and energetically optimized using Marvin Sketch with 221+ as the force field (www.chemaxon.com), prepared, and docked with the same parameters as those of the control docking.

Chemistry. All reactions were carried out using standard techniques for the exclusion of moisture²⁴ except for those in aqueous media. The progress of the reaction was monitored using TLC on 0.25 mm silica F₂₅₄ and detected under UV light. FTIR spectra were determined using Shimadzu. ¹H NMR and ¹³C NMR spectra were determined using a Bruker spectrometer (700 MHz) with TMS as an internal standard, and the mass spectra were determined using a QP2010S Shimadzu with EI 70 eV. Melting points were obtained using a STUART SMP electro-thermal apparatus and were uncorrected.

In a round-bottom flask, aniline or its derivative (3.59 mmol) was mixed with pyridine (7.18 mmol) and then added with 3-bromopropionyl chloride (8 mmol). The mixture was stirred for 20–30 min at room temperature. The progress of the reaction was monitored using TLC and color tests using DAB HCl. When the product was formed, the mixture was then washed with Na₂CO₃ 10%, followed by filtration. The solid product was collected and recrystallized using suitable organic solvents (adapted from refs 25–28). The characterization and the NMR spectra of the compounds are presented in the Supporting Information.

In Vitro Fluorescence Binding Assay (FBA). The MMP9 enzyme kit was purchased from Biovision containing lyophilized MMP9, FRET-based MMP9 substrate, MMP9 assay buffer, and NNGH (*N*-isobutyl-*N*-(4-methoxyphenylsulfonfyl) glycidylhydroxamic acid) inhibitor as the positive control. The lyophilized enzyme was reconstituted with 110 µL of 30% glycerol in deionized water. The reconstituted enzyme was diluted into 550 µL of buffer and ready to be used in the assay. The compound sample was prepared by dissolving it in DMSO to have a final concentration of 200 µg/mL in the 96-microwell plate. The final concentration of DMSO in each well was less than 2%. Each sample (1 µL) was well mixed with the buffer (44 µL), followed by addition of the enzyme (5 µL) into each well. The mixture was then incubated at 37 °C for 30 min. The substrate (50 µL; 40 µM) was added to the mixture and then reincubated at 37 °C for 60 min. The fluorescence was read using a Tecan Infinite Pro200 Microplate Reader at 325/393 nm (adapted from refs 29 and 30).

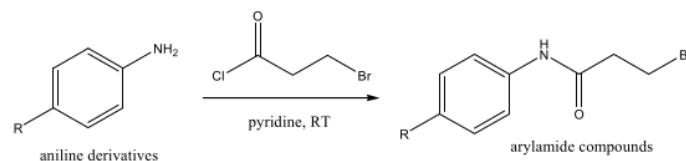
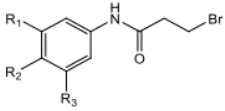
In Vitro Gelatin Zymography Assay (A). The 4T1 metastatic cell line (ATCC CRL 2539) was cultured in Dulbecco's Modified Eagle Medium (DMEM; Gibco) with 10% Fetal Bovine Serum (Gibco), 1% PenicillinStreptomycin (Gibco), and 0.5% fungizone (Gibco). The 4T1 cells (1×10^6) were seeded into each well of a six-well plate and incubated at 37 °C in a CO₂ incubator for 24 h. Cells were incubated with a 10 µM sample, in a serum-free medium for 24 h. The medium

was collected and subjected to polyacrylamide gel electrophoresis (PAGE) on a 10% SDS-PAGE gel containing 0.1% gelatin and run in the SDS running buffer. The gels were washed in a renaturing solution containing 2.5% Triton X-100 for 30 min, then incubated with a buffer (50 mM Tris-HCl, 150 mM NaCl, 10 mM CaCl₂) for 20 h at 37 °C. The gels were stained using 0.5% Coomassie Brilliant Blue and incubated for 30 min at RT and destained with a destaining solution (10% v/v methanol and 5% v/v acetic acid). Gels were then scanned and analyzed with image-J software.^{31,32} Pentagamavunone-1 ((2*E*,5*E*)-2-[(4-hydroxy-3,5-dimethylphenyl)methylidene]-5-[(3-methoxy-4,5-dimethylphenyl)methylidene]cyclopentanone) was used as the positive control.³³

In Vitro MTT Cytotoxicity Assay. 4T1 and Vero cell cytotoxicity were determined using the MTT assay: Cells were seeded into wells with a volume of 100 µL (10^4 cells) per well and checked under an inverted microscope to see the distribution. Cells were then incubated under a CO₂ atmosphere overnight until returned to normal conditions and were then ready to be used. The normal cells in the plate were then taken from the incubator, and the media were discarded. The concentration series of the sample in 0.1% DMSO was seeded into the well and then incubated under a CO₂ atmosphere for 24 h. The media were then removed, and 100 µL of MTT reagent (0.5 µg/mL) was applied per well followed by incubation under a CO₂ atmosphere for 4 h until the formazan was formed. The reaction was then stopped by adding 100 µL of 10% SDS in 0.1 N HCl. The plate was then wrapped using aluminum foil and stored in a dark room at room temperature overnight. Absorbance was read using the Tecan Infinite Pro200 Microplate Reader at 595 nm (adapted from ref 34). Doxorubicin was added to the cultures at the following concentrations: 0, 2.5, 5, 10, 20, and 40 µg in a final volume of 100 µL as a positive control using DMSO 0.1%.

Molecular Dynamics. The interactions of three compounds with PEX9 were further investigated by MD simulation, which are two active compounds (7 and 9) and the least active compound (4), simulated for comparison. AMBER16 was utilized to perform geometry minimization and MD simulation in an explicit TIP3P water model.² First, minimization was done by using 1000 steps each for steepest descent and conjugate gradient, respectively. The MD system was gradually heated to 310 K over 60 ps in the NVT ensemble. A harmonic restraint of 5 kcal/mol Å² on the complex was used in the heating stage, followed by a 1 ns of NPT equilibration. During the equilibration stage, the harmonic restraint was gradually reduced by 1 kcal/mol Å² until it reached zero. Finally, the production run in the NPT ensemble was carried out for 100 ns. The time step for the production run was 2 fs with the use of the SHAKE algorithm. A Langevin thermostat was used to control the temperature, where the collision frequency parameter was set to 1 ps⁻¹. A Berendsen barostat was used to control the pressure, where the coupling constant and target pressure were set to 1 ps and 1 bar, respectively. The cutoff value for nonbonded interactions was set to 9 Å. Particle Mesh Ewald was activated to treat long-range electrostatic interactions. Cpptraj in AmberTools was used to analyze the MD trajectories.³⁵ The binding energy between the compounds and PEX9 was computed using the MM/PBSA (Molecular Mechanics/Poisson–Boltzmann Surface Area) method implemented in the MMPBSA.py program of AMBER16. The calculation of binding energy was calculated

Scheme 2. Reaction of Aniline Derivative with 3-Bromopropionyl Chloride to Produce Arylamide Derivatives

Table 1. Docking Results of the 10 Arylamide Compounds Presenting the Amino Acid Residues Being Involved in the Interaction and Its Estimated K_i


ligand	R_1	R_2	R_3	$\Delta G_{\text{bind}}(\text{kcal/mol})$	amino acid residues	estimated $K_i(\mu\text{M})$
1	H	H	H	-6.40	GLN154	20.52
2	H	NO ₂	H	-6.95	GLU14, ARG106	8.05
3	H	Cl	H	-6.76	GLN154	8.56
4	H	F	H	-6.40	GLN154	20.30
5	H	COOC ₂ H ₅	H	-7.09	GLU14, ARG106	6.31
6	H	SO ₂ NH ₂	H	-7.57	GLU14, GLU60, ALA104	2.83
7	H	SO ₂ NH-pyrimidine	H	-9.09	ARG106, GLU14	0.22
8	H	SO ₂ NH-4-methylpyrimidine	H	-8.88	ARG106, GLN154, GLU157	0.33
9	H	SO ₂ NH-4,6-dimethylpyrimidine	H	-9.38	ARG106, GLU14, GLN154	0.13
10	OCH ₃	OCH ₃	OCH ₃	-6.67	GLU14, GLU60, ARG106	48.49

from the addition of molecular mechanical (MM) energy change in the gas phase and solvation free energy. The MM energy was composed of internal energy, the Coulomb electrostatic term, and the van der Waals interaction term, whereas the solvation free energy was composed of electrostatic and nonelectrostatic solvation energy.

RESULT

Molecular Docking and Synthesis Design. The design was initiated from an arylamide ring that was predicted to contribute to the inhibition of PEX9 activity.¹⁷ Although diverse functional groups have been suggested to be substituted at the *para* position of the ring to study the structure–activity relationships, their contribution, however, was not discussed.¹⁸ Therefore, we are interested in exploring these contributions in terms of the binding to PEX9 via a docking study. Previously, an active arylamide that had OCHF₂ attached to the *p*-position demonstrated that the electron-withdrawing group (EWG), F₂, and CH (steric group) might be responsible for PEX9 inhibition (Dufour et al.). Thus, we hypothesize that attaching the electron-withdrawing group (EWG) together with a steric functional group at the *p* position will increase the arylamide activity. In this study, we attached EWG, i.e., nitro (NO₂ = 2), chloro (Cl = 3), and fluoro (F = 4), and EWG plus a steric/hydrophobic group, such as ethylaceto (COOC₂H₅ = 5), sulfonamide (SO₂NH₂ = 6), sulfonamide-pyrimidine (7), sulfonamide methylpyrimidine (8), sulfonamide dimethylpyrimidine (9), at *p*-arylamide. We also designed a compound that has an electron-donating group (EDG) with a steric/hydrophobic character (OCH₃ = 10) attached at the 3, 4, and 5 positions, to investigate whether EDG plus a steric character could also contribute to the inhibition of PEX9 activity. As a control, arylamide (1) with no

substitution at the *p* position was also synthesized for the study. The reaction is presented in Scheme 2.

Docking of the sulfate ion as the control ligand into PEX9 showed an RMSD of 1.69 Å (less than 2.0 Å), indicating the docking parameters are reproducible.²³ Table 1 shows the docking results where the free energy of binding (ΔG_{bind}) of all the compounds studied is less than -6 kcal/mol (-6.40 to -11.36 kcal/mol), predicting the ability of the ligands to bind competitively with the substrate into PEX9's binding site. Most ligands displayed hydrogen bond interaction with GLU14, GLU60, ARG106, ASP151, and GLN154 of the PEX9's binding site. Thus, these compounds have proceeded for the synthesis.

Chemistry. The synthetic products showed a negative colorimetric reaction with dimethylamino benzaldehyde HCl (DAB HCl), indicating that the nucleophilic acyl substitution (S_NA) has taken place. It has been well documented that free aromatic amine reacts with DAB HCl, forming an orange color describing a Schiff base reaction to produce an imine ($-\text{CH}=\text{N}-$). The arylamide products were then confirmed for their purity using TLC, showing a pure single spot. The presence of a carbonyl functional group was confirmed by FTIR, showing a very strong stretching band near 1500 cm^{-1} . The proton NMR demonstrates aromatic protons which vary in chemical shifts depending on the chemical environment, but most of them are deshielded at 6–8 ppm. The ethylene proton is confirmed by the presence of two triplet signals near 2.7 and 3.3 ppm. The confirmation of the Br group, as well as the whole structure, was carried out using mass spectroscopy. For compounds with a sulfonamide functional group, the mass/ion was not observed in the parent molecule. However, there is always a 65 mass/ion deduction due to the rearrangement of the amine group to attach the arylamide ring at the *p* position when the SO₂ is fragmented.³⁶ Following the confirmation of the structures of

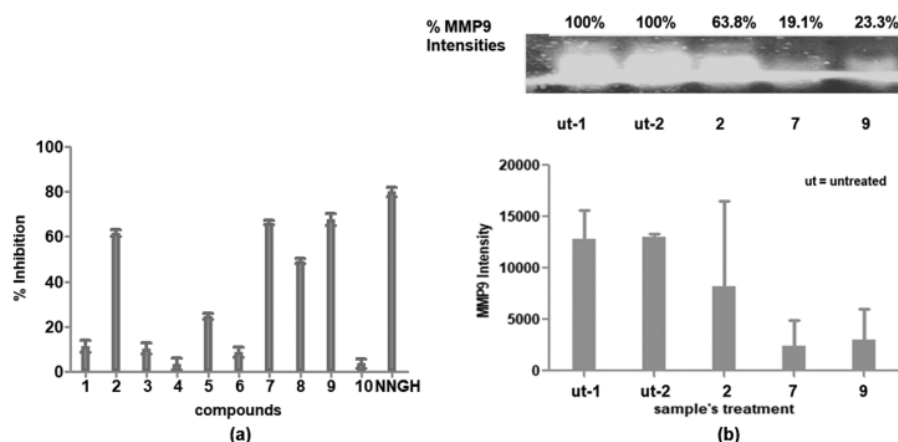


Figure 2. (a) The % inhibition of the 10 arylamide compounds against MMP9 *in vitro* using FBA and (b) the zymogram of MMP9 expressed by 4T1 determined using GZA with the untreated cells and the treated cell by 2, 7, and 9.

the 10 synthesized compounds, bioactivity against MMP9 *in vitro* was carried out.

In Vitro Fluorescence Binding Assay. In the *in vitro* binding assay, MMP9 is reacted with its substrate to perform proteolysis. The substrate is a peptide linked to the fluorophore, cleaved by MMP9, leading to fluorescence, which can be measured spectrophotometrically as the enzyme activity.^{37,38} The presence of a synthetic compound should reduce the fluorescence, indicating the inhibition of MMP9-substrate binding. In this study, the tested compounds demonstrated 4 to 68% inhibition at 200 $\mu\text{g/mL}$ (Figure 2). High percentages of inhibition are exhibited by 2 (67%), 7 (66%), and 9 (68%), whereas the other seven compounds showed less than 50% inhibition. The moderate to low activities were performed by 8 (49%), 5 (25%), 1 (11%), 3 (10%), 6 (9%), and 4 and 10 (both were 4%). These results indicate that arylamide compounds can inhibit the activity of MMP9 from low to high potency. Interestingly, compounds with sulfonamide-pyrimidine substitutions at the *para* position perform higher inhibitory activities with % inhibition = 66 and 68 for nonmethylated (6) and dimethylated pyrimidine (8), respectively. In addition, the *p*-nitro substituted compound (2) also demonstrates a high percentage of inhibition (67%) against MMP9. Sulphonamide and nitro groups are two strong electron-withdrawing groups, thus strengthening our hypothesis on the role of EWG in MMP9 inhibition. Compound 9 with the highest percentage of inhibition was then rerun for its IC_{50} experiment, calculating a micromolar concentration of 70 μM . Although the IC_{50} of 9 was not as potent as NNGH (47.80 nM) as a positive control 9 could, however, be less toxic than NNGH. It was well studied that a MMP9 inhibitor with a hydroxamate-like structure fails in clinical studies due to its nonselective inhibition toward the catalytic site.¹⁴

In Vitro Gelatin Zymography Assay (GZA). 4T1, a triple-negative breast cancer cell line from *Mus musculus*, was used to test the gelatinase activity of the samples. Alignment of amino acid sequences between hemopexin MMP9 expressed by MDA-MB-231 from humans and MMP9 from 4T1 of *Mus musculus* demonstrated 61% identity. The high homology between the two MMP9s suggested that 4T1 could be used as a cell model to express MMP9. The sequence alignment of

PEX9 (PDB 1ITV) with MMP9 from *Mus musculus* is presented in Figure S1 (Supporting Information).

Gelatin zymography is a simple method to determine the inhibitory activity of a compound against MMP9.³⁹ In this experiment, 4T1 cells expressing MMP9 can be detected using electrophoresis. MMP9 will precede gelatinolysis during electrophoresis and show its existence as a transparent band with a blue background in the absence of gelatinolysis.⁴⁰ The band is assigned as a 100% intensity of MMP9 being expressed by a 4T1 cell. In the presence of an MMP inhibitor, the intensity should be reduced, indicating the inhibition of such an inhibitor in MMP9 gelatinolytic activity.⁴¹

Figure 2b presents a zymogram of MMP9 expressed by 4T1 cells consisting of five bands: untreated cell 1; untreated cell 2; and cells treated by 2, 7, and 9 at a 10 μM concentration. It is clear that the band intensity of the untreated 4T1 cells is different than that of the 4T1 cells treated with those three active compounds, indicating that 2, 7, and 9 have inhibited the activity of MMP9. As presented in Figure 2b, the average intensity of untreated cell 1 is 12947.3, whereas, in the cells treated with 2, the band intensity is reduced to 8266.2. The treated cells showed reducing activity down to 63.8% compared to the control cell, indicating that MMP9 was inhibited by 2 up to 36.2%. Interestingly, the activity of MMP9 was reduced by 7 and 9 down to 19.1% and 23.3%, respectively, indicating that these two most active compounds inhibited 80.9% and 76.7% of the MMP9 gelatinolytic activity, respectively. These data support the initial findings using a fluorescence assay that 2, 7, and 9 were able to inhibit the activity of MMP9. PGV-1, as the positive control, showed 35.39% inhibition toward gelatinolysis at a concentration of 2 μM . In respect to the concentration used by 2, 7, and 9, the concentration of the positive control was 5 times lower than that of the tested compounds. Therefore, we could assume that when they were at the same concentration, the positive control could be more potent than the tested compounds.

In Vitro MTT Cytotoxicity Assay. The toxicity of the three compounds was tested toward 4T1 cells as well as normal Vero cells to determine the safety and selectivity of the compounds. To assess the cell metabolic activity, the MTT assay was carried out. The number of viable cells present was reflected by NAD(P)H-dependent oxidoreductase enzymes

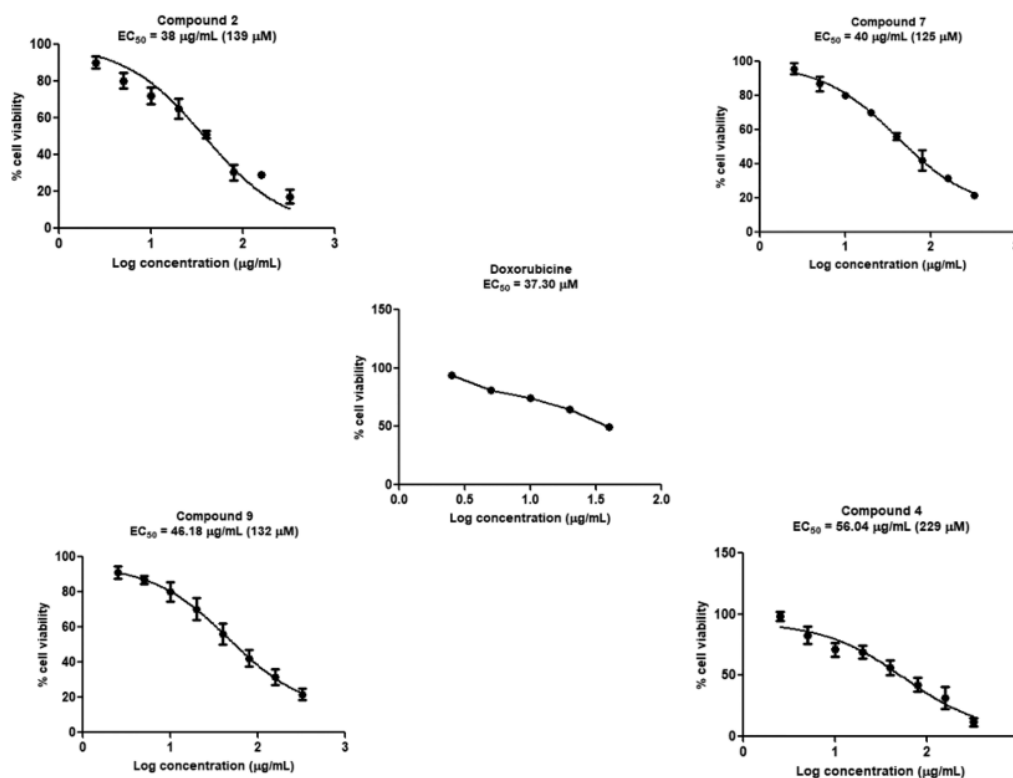


Figure 3. Drug-dose-dependent curves of 2, 7, 9, and 4 against 4T1 cell growth.

Table 2. Summary of the Arylamide Activities in Inhibiting MMP9, MMP9 Being Expressed by the 4T1 Cell, the 4T1 Cell, and the Normal Vero Cell As Well As the ΔG_{bind} of the Docking Study

compounds	% inhibition on MMP9 (FBA)	% inhibition on MMP9 (GZA)	EC_{50} on 4T1 cell (μM)	CC_{50} on vero Cell (μM)	safety index (CC_{50}/EC_{50})	ΔG (kcal/mol)
1	11					-6.40
2	67	36.20	139	389	2.80	-6.95
3	10					-6.76
4	4		229	1073	4.68	-6.40
5	34					-7.09
6	9					-7.57
7	66	80.90	125	269	2.15	-9.09
8	49					-8.88
9	68	76.70	132	763	5.80	-9.38
10	4					-6.67
NNGH	80					
PGV-1 (2 μM)		35.39				
doxorubicin			37.30	211.30	5.66	

under defined conditions. The reduction of tetrazolium dye MTT 3-(4,5-dimethylthiazol-2-yl)-2,5-diphenyltetrazolium bromide formed a purple color via the enzyme in the soluble formazan product. The cell was then solubilized by an organic solvent such as DMSO while releasing a soluble formazan, which was measured spectrophotometrically. Since the reduction of MTT can only occur in metabolically active cells, the level of activity is a measure of viability of the cell.⁴² Figure 3 illustrates the drug-dose-dependent curves for the three active compounds (2, 7, and 9) and an inactive compound (4) against 4T1 cells.

The assay system well worked by showing the positive control inhibited 50% of cell growth at 37.30 μM . All the three compounds have effective concentrations to inhibit the 4T1 cell growth within a narrow range (125–139 μM), with the best EC_{50} exhibited by 7 (EC_{50} = 125 μM), followed by 9 (EC_{50} = 132 μM) and 2 (EC_{50} = 139 μM). Although 4 showed only 4% inhibition in the MMP9 fluorescence binding assay, the EC_{50} of the compound in the cellular assay is 229 μM .

Figure S2 (Supporting Information) illustrates the morphology of the Vero cell before and after treatments using 7. The cell size is smaller than its normal size and shrank because of

the loss of cytoplasmic fluid due to the membrane disruption, as shown by the detached cell upon the compound's treatment. All three compounds showed a high CC_{50} on the Vero cells. A compound which has a concentration to stop at least 50% of noncancer cell growth for more than 10 μ M is categorized as nontoxic.^{43,44} Thus, the three most active compounds against MMP9 are also relatively safe for further development, as confirmed by the calculated safety index (SI).

The safety index (SI) is a ratio of CC_{50} to EC_{50} in which the higher the value of the SI, the less toxic the compound would be. The results showed that among three compounds, the SI was calculated as followed: $9 > 4 > 2 > 7$. Therefore, the safest compound is 9 with $SI = 5.80$. Table 2 is the summary of the arylamides' activities in inhibiting MMP9, MMP9 being expressed by 4T1 cells, 4T1 cells, and the normal Vero cells. The trend seemed similar to the assay using either FBA or GZA, and when compared to the positive control, the tested compounds were still less potent. However, we still hope that in further studies, 9 could be less toxic than doxorubicin.

Molecular Dynamics Study. MD simulation was performed to investigate further the interaction of the active inhibitors, 7 and 9, with the MMP9 binding site. It is noted that 7 and 9 are very similar, only different by the two methyl groups on the pyrimidine ring. The RMSD profile of these two compounds during the simulation showed that 7 is more stable than 9 in the binding site of PEX9 (Figure 4).

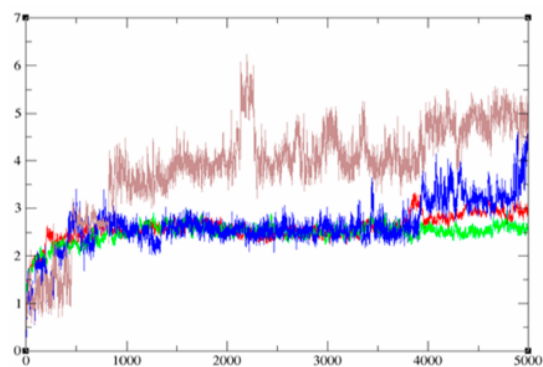


Figure 4. RMSD of 7 (blue) and 9 (brown) in the PEX9 (green and red, respectively) during 100 ns of MD simulation, presented in 5000 frames.

The simulation result suggested that the high affinity of 7 and 9 in the PEX9 is due to the conserved H-bond with ARG106 (Figure 5). Nevertheless, the binding mode between 7 and 9 (Figure 5a and b, respectively) with ARG106 is different. It is shown that the sulfonamide group of 9 is more oriented toward ARG106 as compared to that of 7. This observation is supported by the time-dependent distance between ARG106 and the H-bond acceptor of the ligand (Figure 5d), indicating that the H-bond between 7 and ARG106 was conserved for 60 ns of simulation, whereas that of 9 was stable until the end of the simulation.

The least active compound 4 is also simulated for comparison purposes. It is shown that the binding mode of 4 is quite different from the two most active ones. The bromo group of 4, unlike the other two, is oriented outside the binding site (Figure 5c). In this study, the addition of EWG is

expected to improve the inhibition activity by participating in the interaction with PEX9. Therefore, the orientation of the bromo group outside the binding site of PEX9 could explain the least activity of 4 compared to the other compounds.

The MM/PBSA binding energy of 7 (−8.03 kcal/mol) is lower than 9 (−6.41 kcal/mol), suggesting that 7 has a stronger binding with PEX9 than 9 (Table 1). This result agrees with the higher stability of 7 in the enzyme's binding site, as depicted by the RMSD values over 100 ns (Figure 4). Moreover, the least activity of 4 is implied by the highest binding energy (−3.34 kcal/mol) as compared to 7 and 9.

Table 3 shows the binding energy decomposition of compounds 7, 9, and 4 in the binding site of PEX9. The electrostatic term represents the H-bond occupancy between the ligands and receptor. In agreement with the binding mode and H-bond analysis, 7 has stronger electrostatic energy than 9. Interestingly, the electrostatic energy of 9 is higher than that of the least active compound 4. However, hydrophobic interaction formed by 7 and 9, which was represented by van der Waals and surface area terms (nonpolar solvation + dispersion), was stronger than that of 5; therefore, it can be suggested that hydrophobic interaction plays an important role in stabilizing the ligand at the PEX9 binding site, besides the electrostatic interaction. Nevertheless, it can be suggested that the stabilization of the ligand inside the binding site of PEX9 is also contributed by the H-bond formation with ARG106. Table 3 also shows that the occupancy of the H-bond of 7 and 9 with ARG106 is higher than 4.

DISCUSSION

In this study, we have shown that the arylamide scaffold is the backbone that binds to the cavity of PEX9 while interacting with the surrounding important amino acids. Without any substitution at the *para* position, 1 could inhibit MMP9, albeit with a low percent inhibition. In contrast, locating EWG, such as ethylaceto (5) and sulfonamide (6), increases the activities back. The characters of EWG in 7, 8, and 9 are observed by an adjoining pyrimidine ring to $NH-SO_2$. In addition, the steric character is increased by the addition of the methyl (8) and dimethyl group (9) to the pyrimidine ring, thus contributing to more pronounced inhibition toward MMP9 activity. The attachment of halogen EWG such as chloro (3) and fluoro (4) did not improve the binding with PEX9 as shown in the docking study, where only one hydrogen bond interaction with GLN154 is stabilizing the interaction between the ligands and PEX9, thus contributing to the higher free energy of binding. This result is supported by the *in vitro* studies where the two halogenated arylamides are found inactive. Thus, we suggested that there is a need for the addition of a steric group at this position. Although halogen is EWG, the EWG strength, however, is considered moderate.⁴⁵ Thus, it is insufficient to possess the inhibition of the enzyme. This result strengthens the hypothesis that a strong EWG with steric characters would increase the activity of arylamide in inhibiting MMP9. Attaching EDG together with a steric character such as OCH_3 at the 4, 5, and 6 positions (10) decreases the activity.

Compound 2 was designed with a relatively low free energy of binding (−6.95 kcal/mol), implying its potential to interact with PEX9 strongly. In fact, these compounds interact with ARG106 via H-bond interactions (Figure 6), which was also seen with the sulfate ion in the control docking. The *in vitro* assay using the fluorescence method agrees with the prediction using the *in silico* method, that compound 2 inhibits the

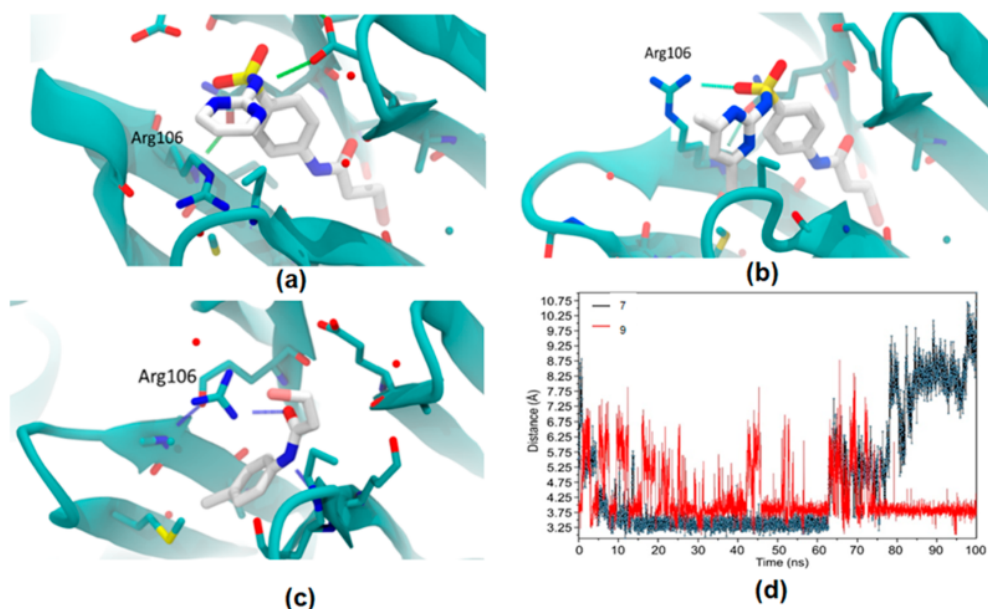


Figure 5. Hydrogen bond formation between (a) 7, (b) 9, and (c) 4 with ARG106 and (d) the distance between the guanidino group of ARG106 and the closest hydrogen bond acceptor of the ligand (7 and 9) during 100 ns of MD simulation.

Table 3. Decomposition of Binding Energy Using MM/PBSA Method and H-Bond Occupancy with ARG106 Throughout the MD Simulation

binding energy component	compound (kcal/mol)		
	7	9	4
van der Waals	-49.88 ± 1.25	-48.92 ± 0.59	-27.96 ± 0.53
electrostatic	-37.17 ± 1.80	-19.76 ± 0.86	-27.93 ± 1.59
electrostatic solvation (PB)	56.16 ± 1.21	38.93 ± 0.52	38.96 ± 1.56
nonpolar solvation	-30.77 ± 0.16	-32.57 ± 0.30	-20.35 ± 0.30
dispersion	53.64 ± 0.18	55.91 ± 0.21	33.93 ± 0.22
gas binding energy	-87.05 ± 1.42	-68.68 ± 1.32	-55.89 ± 1.40
solvated binding energy	79.03 ± 1.32	62.27 ± 0.77	52.55 ± 1.79
total binding energy	-8.03 ± 2.05	-6.41 ± 1.13	-3.34 ± 1.67
H-bond occupancy with ARG 106	49%	50%	27%

proteolytic activity of MMP9 toward the peptide substrate. This result is further supported by the results of the gelatin zymographic assay (GZA), where **2** also inhibits the gelatinolytic activity of MMP9 expressed in the 4T1 cells by as much as 36.2%. Interestingly, **2** is also less cytotoxic to the Vero cell lines as compared to **7**.

Because the activity of **2** is lower than that of **7** and **9** in GZA, we did not study the dynamic behavior of **2** via MD simulation. However, docking results predicted that **2** interacts with PEX9 via H-bond interactions with ARG106 and GLU14 by O-nitro and O-carbonyl, respectively. The H-bond between O-nitro with ARG106 showed strong EWG character at the *para* position of arylamide as indicated by the distance of the H bond (1.9 Å).

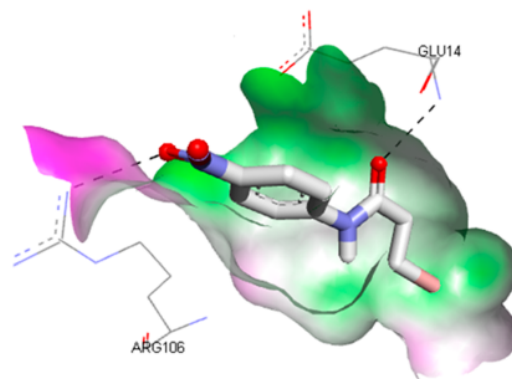


Figure 6. Docked pose of **2** at the binding site of PEX9. The H-bond interaction is visualized as a black dashed line.

Compounds **7** and **9** are expected to bind more selectively in the hemopexin-like domain (PEX9) than in the catalytic domain. The expected molecular mechanism is via interruption of the homodimerization of two PEX9 monomers at blade 4 via hydrophobic interactions. When the homodimerization of PEX9 is interrupted, its binding to the lipoprotein-related protein-1 (LRP-1) receptor is also disrupted; therefore, there is no signal transduction to an extracellular-signal-regulated kinase (ERK1/2) and Akt, to lead the cell migration.⁴⁶ On the other hand, the binding of the inhibitor to the PEX9 will act as an allosteric inhibitor to interrupt the proteolysis of ECM, which holds the Vascular Endothelial Growth Factor (VEGF). Hence, there is no VEGF binding into its receptor at the membrane to proceed with the angiogenesis.

MD simulation showed that the ligand-binding with important residues at the active site plays an important role

in stabilizing the interaction. MD simulation has been used for evaluating the stability of ligand binding predicted by docking.⁴⁷ It is shown that low binding energy predicted in docking does not always indicate stable interaction. Thus, it must be further studied by dynamic simulation. Sulfone compounds have been reported having MMP9 inhibition activity at a nanomolar concentration, which includes bis-arylsulfonamide hydroxamate,⁴⁸ arylsulfone,⁴⁹ biaryl ether sulfonamide⁶ and ¹¹C-radiolabeled sulfonamide.⁵¹ However, there is no further study on the binding selectivity of these compounds toward MMP9. To the best of our knowledge, the study of arylamide incorporated with sulfonamide as an MMP9 inhibitor and its dynamic behavior toward the PEX9 binding site has not been reported elsewhere. However, there is still a need to confirm the selectivity of compounds toward the hemopexin domain in MMP9 using a blue shift in the pro-MMP9 tryptophan fluorescence assay. The compound has moderate activity, but it has potential to be developed for the newly discovered moderate inhibitors, which are a step toward discovering highly potent MMP9 inhibitors in the future.

In addition, it would be challenging to study the chemical mechanism of the rate limiting step of the MMP9. The comparison between the transition state structure and the structure of the studied ligands will give more understanding of why the studied ligand showed either active or inactive inhibition toward MMP9. The study could be initiated using molecular docking of the ligand with MMP9 and followed by MD simulation. The best complex of the ligand in the binding site of the protein proceeded for QM to calculate the energy of binding from the initial state, transition state, and the product state. The calculation could explain the reaction barriers (rate of limiting step) for the transformation of the ligand and which protonation state could be thermodynamically more favorable between two different ligands. The proposed chemical mechanism was different from the current mechanism in which the addition reaction from the essential residue of the protease to the ligand was more favorable than the deprotonation of the ligand.^{52–54}

CONCLUSION

In the present study, we developed a number of arylamide compounds expected to be more selective toward MMPs by inhibiting the hemopexin domain of the enzyme. Compounds 2 (3-bromo-N-(4-nitrophenyl)propanamide), 7 (3-bromo-N-{4-(4,6-dimethylpyrimidin-2-yl)sulfamoyl}phenyl)propanamide), and 9 (3-bromo-N-{4-[(4,6-dimethylpyrimidin-2-yl)sulfamoyl]-phenyl}propanamide) showed the most potent activities compared to the other seven synthesized arylamides. The results showed an agreement between the *in silico* study (molecular docking and molecular dynamics, which were used as tools in the design and rationalization of the molecular behavior of the arylamide) and the *in vitro* study via fluorescence and gelatin zymographic assays.

ASSOCIATED CONTENT

Supporting Information

The Supporting Information is available free of charge at <https://pubs.acs.org/doi/10.1021/acs.jcim.9b00630>.

The structural characterization and the NMR spectra of the synthesized compounds; (Figure S1) the sequence alignment of amino acid sequences between hemopexin MMP9 expressed by MDA-MB-231 from human and

MMP9 from 4T1 of *Mus musculus*; and (Figure S2) the morphology of the Vero cell before and after treatments using 7 (PDF)

AUTHOR INFORMATION

Corresponding Author

*E-mail: mhariono@usd.ac.id. Phone: +627488303 or +6274883968. Fax: +6274886529.

ORCID

Maywan Hariono: 0000-0001-6757-2116

Muhammad Yusuf: 0000-0003-1627-1553

Habibah A. Wahab: 0000-0002-8353-8679

Author Contributions

The authors declare no competing financial interest.

Author Contributions

M.H. designed and supervised this study as the final project of K.C.P., E.S.N., Y.K.W., S.P.D., B.W.J., and R.T.'s Bachelor of Pharmacy, in collaboration with H.A.W. Docking and synthesis were carried out by K.C.P., E.S.N., Y.K.W., S.P.D., B.W.J., and R.T. under J.J.'s supervision. R.F.N. performed the enzymatic studies, whereas the cellular assays were performed by R.R. Gelatin zymography assays were performed by R.D.R. and L.Q. under R.I.J.'s supervision. MD was set up, simulated, and analyzed by M.Y. and B.A.-N.

Funding

This study is funded by Indonesia Toray Science Foundation (ITSF) 2017–2018 and Sanata Dharma University through research grant no. 026/Penel./LPPM-USD/4/2018.

Notes

The authors declare no competing financial interest.

ACKNOWLEDGMENTS

M.H. acknowledges the Central Laboratory of Padjadjaran University, Indonesia for facilitating the MMP9 experiment. R.I.J. acknowledges Prof. Dr. Mashashi Kawaichi (NAIST), Japan for his kind donation of the 4T1 cell in GZA. H.A.W. acknowledges the support from Universiti Sains Malaysia's Research University Grant (1001/PFARMASI/870031) that enabled this collaborative work.

REFERENCES

- (1) Nagai, H.; Kim, Y. H. Cancer prevention from the perspective of global cancer burden patterns. *J. Thorac. Dis.* **2017**, *9*, 448–451.
- (2) Zahreddine, H.; Borden, K. Mechanisms and insights into drug resistance in cancer. *Front. Pharmacol.* **2013**, *4*, 1–8.
- (3) Housman, G.; Byler, S.; Heerboth, S.; Lapinska, K.; Longacre, M.; Snyder, N.; Sarkar, S. Drug resistance in cancer: an overview. *Cancers* **2014**, *6*, 1769–1792.
- (4) Carels, N.; Spinassé, L. B.; Tilli, T. M.; Tuszyński, J. A. Toward precision medicine of breast cancer. *Theor. Biol. Med. Modell.* **2016**, *13*, 1–46.
- (5) Yao, H.; He, G.; Yan, S.; Chen, C.; Song, L.; Rosol, T. J.; Deng, X. Triple-negative breast cancer: is there a treatment on the horizon? *Oncotarget* **2017**, *8*, 1913–1924.
- (6) Roberti, M. P.; Arriaga, J. M.; Bianchini, M.; Quintá, H. R.; Bravo, A. I.; Levy, E. M.; Mordoh, J.; Barrio, M. M. Protein expression changes during human triple negative breast cancer cell line progression to lymph node metastasis in a xenografted model in nude mice. *Cancer Biol. Ther.* **2012**, *13*, 1123–1140.
- (7) Hariono, M.; Yuliani, S. H.; Istyastono, E. P.; Riswanto, F. D.; Adhipandito, C. F. Matrix metalloproteinase 9 (MMP9) in wound healing of diabetic foot ulcer: Molecular target and structure-based drug design. *Wound Med.* **2018**, *22*, 1–13.

- (8) Jabłońska-Trypuc, A.; Matejczyk, M.; Rosochacki, S. Matrix metalloproteinases (MMPs), the main extracellular matrix (ECM) enzymes in collagen degradation, as a target for anticancer drugs. *J. Enzyme Inhib. Med. Chem.* **2016**, *31*, 177–183.
- (9) Roy, S.; Pramanik, A.; Chakraborti, T.; Chakraborti, S. Multifaceted Role of Matrix Metalloproteinases on Human Diseases. In *Proteases in Human Diseases*; Springer, 2017; pp 21–40.
- (10) Vandooren, J.; Van den Steen, P. E.; Opdenakker, G. Biochemistry and molecular biology of gelatinase B or matrix metalloproteinase-9 (MMP-9): the next decade. *Crit. Rev. Biochem. Mol. Biol.* **2013**, *48*, 222–272.
- (11) McCarthy, S. M.; Bove, P. F.; Matthews, D. E.; Akaike, T.; van der Vliet, A. Nitric oxide regulation of MMP-9 activation and its relationship to modifications of the cysteine switch. *Biochemistry* **2008**, *47*, 5832–5840.
- (12) Nagase, H.; Visse, R.; Murphy, G. Structure and function of matrix metalloproteinases and TIMPs. *Cardiovasc. Res.* **2006**, *69*, 562–573.
- (13) Cathcart, J.; Pulkoski-Gross, A.; Cao, J. Targeting matrix metalloproteinases in cancer: bringing new life to old ideas. *Gen Dis* **2015**, *2*, 26–34.
- (14) Vandenbroucke, R. E.; Libert, C. Is there new hope for therapeutic matrix metalloproteinase inhibition? *Nat. Rev. Drug Discovery* **2014**, *13*, 904–927.
- (15) Rosenblum, G.; Van den Steen, P. E.; Cohen, S. R.; Grossmann, J. G.; Frenkel, J.; Sertchook, R.; Slack, N.; Strange, R. W.; Opdenakker, G.; Sagi, I. Insights into the structure and domain flexibility of full-length pro-matrix metalloproteinase-9/gelatinase B. *Structure* **2007**, *15*, 1227–1236.
- (16) Fingleton, B. MMPs as therapeutic targets—still a viable option? In *Seminars in Cell & Developmental Biology*, 2008; Elsevier, 2008; Vol. 19; pp 61–68.
- (17) Dufour, A.; Sampson, N. S.; Li, J.; Kescu, C.; Rizzo, R. C.; DeLeon, J. L.; Zhi, J.; Jaber, N.; Liu, E.; Zucker, S.; Cao, J. Small-molecule anticancer compounds selectively target the hemopexin domain of matrix metalloproteinase-9. *Cancer Res.* **2011**, *71*, 4977–4988.
- (18) Alford, V. M.; Kamath, A.; Ren, X.; Kumar, K.; Gan, Q.; Awwa, M.; Tong, M.; Seeliger, M. A.; Cao, J.; Ojima, I.; Sampson, N. S. Targeting the hemopexin-like domain of latent matrix metalloproteinase-9 (proMMP-9) with a small molecule inhibitor prevents the formation of focal adhesion junctions. *ACS Chem. Biol.* **2017**, *12*, 2788–2803.
- (19) Fields, G. B. New strategies for targeting matrix metalloproteinases. *Matrix Biol.* **2015**, *44*, 239–246.
- (20) Ugarte-Berzal, E.; Bailón, E.; Amigo-Jiménez, I.; Vituri, C. L.; del Cerro, M. H.; Terol, M. J.; Albar, J. P.; Rivas, G.; García-Marco, J. A.; García-Pardo, A. A 17-residue sequence from the matrix metalloproteinase-9 (MMP-9) hemopexin domain binds $\alpha 4 \beta 1$ integrin and inhibits MMP-9-induced functions in chronic lymphocytic leukemia B cells. *J. Biol. Chem.* **2012**, *287*, 27601–27613.
- (21) Cha, H.; Kopetzki, E.; Huber, R.; Lanzendörfer, M.; Brandtetter, H. Structural basis of the adaptive molecular recognition by MMP9. *J. Mol. Biol.* **2002**, *320*, 1065–1079.
- (22) Morris, G. M.; Huey, R.; Lindstrom, W.; Sanner, M. F.; Belew, R. K.; Goodsell, D. S.; Olson, A. J. AutoDock4 and AutoDockTools4: Automated docking with selective receptor flexibility. *J. Comput. Chem.* **2009**, *30*, 2785–2791.
- (23) Hevener, K. E.; Zhao, W.; Ball, D. M.; Babaoglu, K.; Qi, J.; White, S. W.; Lee, R. E. Validation of molecular docking programs for virtual screening against dihydropteroate synthase. *J. Chem. Inf. Model.* **2009**, *49*, 444–460.
- (24) Hariono, M.; Ngah, N.; Wahab, H. A.; Abdul Rahim, A. 2-Bromo-4-(3, 4-dimethyl-5-phenyl-1, 3-oxazolidin-2-yl)-6-methoxyphenol. *Acta Crystallogr., Sect. E: Struct. Rep. Online* **2012**, *68*, o35–o36.
- (25) Hariono, M.; Choi, S. B.; Roslim, R. F.; Nawi, M. S.; Tan, M. L.; Kamarulzaman, E. E.; Mohamed, N.; Yusof, R.; Othman, S.; Abd Rahman, N.; Othman, R.; Wahab, H. A. Thioguanine-based DENV-2 NS2B/NS3 protease inhibitors: Virtual screening, synthesis, biological evaluation and molecular modelling. *PLoS One* **2019**, *14*, No. e0210869.
- (26) Abduraman, M. A.; Hariono, M.; Yusof, R.; Rahman, N. A.; Wahab, H. A.; Tan, M. L. Development of a NS2B/NS3 protease inhibition assay using AlphaScreen® beads for screening of anti-dengue activities. *Heliyon* **2018**, *4*, No. e01023.
- (27) Hariono, M.; Wahab, H. A.; Tan, M. L.; Rosli, M. M.; Razak, I. A., 9-Benzyl-6-benzylsulfanyl-9H-purin-2-amine. *Acta Crystallogr., Sect. E: Struct. Rep. Online* **2014**, *70*, o288–o288.
- (28) Valdez, C. A.; Leif, R. N.; Mayer, B. P. An efficient, optimized synthesis of fentanyl and related analogs. *PLoS One* **2014**, *9*, No. e108250.
- (29) Biovision, MMP-1 Inhibitor Screening Kit (Fluorometric). <https://www.biovision.com/mmp-9-inhibitor-screening-kit-fluorometric.html> (accessed on April 5, 2017).
- (30) Adhipandito, C. F.; Ludji, D. P. K. S.; Aprilianto, E.; Jenie, R. I.; Al-Najjar, B.; Hariono, M. Matrix metalloproteinase9 as the protein target in anti-breast cancer drug discovery: an approach by targeting hemopexin domain. *Futur J. Pharm. Sci.* **2019**, *5*, 1–15.
- (31) Hur, S. S.; del Alamo, J. C.; Park, J. S.; Li, Y.-S.; Nguyen, H. A.; Teng, D.; Wang, K.-C.; Flores, L.; Alonso-Latorre, B.; Lasheras, J. C.; Chien, S. Roles of cell confluency and fluid shear in 3-dimensional intracellular forces in endothelial cells. *Proc. Natl. Acad. Sci. U. S. A.* **2012**, *109*, 11110–11115.
- (32) Hames, B. D. *Gel Electrophoresis of Proteins: a Practical Approach*; OUP Oxford, 1998; Vol. 197.
- (33) Meiyanto, E.; Putri, H.; Arum Larasati, Y.; Yudi Utomo, R.; Istighfari Jenie, R.; Ikawati, M.; Lestari, B.; Yoneda-Kato, N.; Nakamae, I.; Kawaichi, M.; Kato, J.-Y. Anti-proliferative and Anti-metastatic Potential of Curcumin Analogue, Pentagamavunon-1 (PGV-1), Toward Highly Metastatic Breast Cancer Cells in Correlation with ROS Generation. *Adv. Pharm. Bull.* **2019**, *9*, 445–452.
- (34) Borra, R. C.; Lotufo, M. A.; Gaglioti, S. M.; Barros, F. d. M.; Andrade, P. M. A simple method to measure cell viability in proliferation and cytotoxicity assays. *Braz. J. Biol.* **2009**, *23*, 255–262.
- (35) Wang, J.; Wolf, R. M.; Caldwell, J. W.; Kollman, P. A.; Case, D. A. Development and testing of a general amber force field. *J. Comput. Chem.* **2004**, *25*, 1157–1174.
- (36) Sun, M.; Dai, W.; Liu, D. Q. Fragmentation of aromatic sulfonamides in electrospray ionization mass spectrometry: elimination of SO₂ via rearrangement. *J. Mass Spectrom.* **2008**, *43*, 383–393.
- (37) Hawkins, K. E.; DeMars, K. M.; Yang, C.; Rosenberg, G. A.; Candelario-Jalil, E. Fluorometric immunocapture assay for the specific measurement of matrix metalloproteinase-9 activity in biological samples: application to brain and plasma from rats with ischemic stroke. *Mol. Brain* **2013**, *6*, 14.
- (38) Lee, J.; Samson, A. A. S.; Song, J. M. Peptide substrate-based inkjet printing high-throughput MMP-9 anticancer assay using fluorescence resonance energy transfer (FRET). *Sens. Actuators, B* **2018**, *256*, 1093–1099.
- (39) Leber, T. M.; Balkwill, F. R. Zymography: a single-step staining method for quantitation of proteolytic activity on substrate gels. *Anal. Biochem.* **1997**, *249*, 24–28.
- (40) Vandooren, J.; Geurts, N.; Martens, E.; Van den Steen, P. E.; Opdenakker, G. Zymography methods for visualizing hydrolytic enzymes. *Nat. Methods* **2013**, *10*, 211–220.
- (41) Ramsby, M. L. Zymographic evaluation of plasminogen activators and plasminogen activator inhibitors. *Adv. Clin. Chem.* **2004**, *38*, 111–133.
- (42) Tolosa, L.; Donato, M. T.; Gómez-Lechón, M. J. General cytotoxicity assessment by means of the MTT assay. In *Protocols in in Vitro Hepatocyte Research*; Springer, 2015; pp 333–348.
- (43) Hughes, J. P.; Rees, S.; Kalindjian, S. B.; Philpott, K. L. Principles of early drug discovery. *Br. J. Pharmacol.* **2011**, *162*, 1239–1249.

- (44) Zhu, T.; Cao, S.; Su, P.-C.; Patel, R.; Shah, D.; Chokshi, H. B.; Szukala, R.; Johnson, M. E.; Hevener, K. E. Hit identification and optimization in virtual screening: practical recommendations based on a critical literature analysis: miniperspective. *J. Med. Chem.* **2013**, *56*, 6560–6572.
- (45) McMurry, J. *Organic Chemistry*, 7th ed.; Brooks/Cole, 2004.
- (46) Cain, C. A bid to revive MMP inhibitors. *SciBX* **2011**, *4*, 701–701.
- (47) Chen, Y.-C. Beware of docking! *Trends Pharmacol. Sci.* **2015**, *36*, 78–95.
- (48) Subramaniam, R.; Haldar, M. K.; Tobwala, S.; Ganguly, B.; Srivastava, D.; Mallik, S. Novel bis-(arylsulfonamide) hydroxamate-based selective MMP inhibitors. *Bioorg. Med. Chem. Lett.* **2008**, *18*, 3333–3337.
- (49) Zhang, Y.-M.; Fan, X.; Yang, S.-M.; Scannevin, R. H.; Burke, S. L.; Rhodes, K. J.; Jackson, P. F. Syntheses and in vitro evaluation of arylsulfone-based MMP inhibitors with heterocycle-derived zinc-binding groups (ZBGs). *Bioorg. Med. Chem. Lett.* **2008**, *18*, 405–408.
- (50) Gooyit, M.; Peng, Z.; Wolter, W. R.; Pi, H.; Ding, D.; Heseck, D.; Lee, M.; Boggess, B.; Champion, M. M.; Suckow, M. A.; Mobashery, S.; Chang, M. A chemical biological strategy to facilitate diabetic wound healing. *ACS Chem. Biol.* **2014**, *9*, 105–110.
- (51) Selivanova, S. V.; Stellfeld, T.; Heinrich, T. K.; Muller, A.; Kramer, S. D.; Schubiger, P. A.; Schibli, R.; Ametamey, S. M.; Vos, B.; Meding, J.; Bauser, M.; Hutter, J.; Dinkelborg, L. M. Design, synthesis, and initial evaluation of a high affinity positron emission tomography probe for imaging matrix metalloproteinases 2 and 9. *J. Med. Chem.* **2013**, *56*, 4912–4920.
- (52) Tao, P.; Fisher, J. F.; Shi, Q.; Vreven, T.; Mobashery, S.; Schlegel, H. B. Matrix metalloproteinase 2 inhibition: combined quantum mechanics and molecular mechanics studies of the inhibition mechanism of (4-phenoxyphenylsulfonyl) methylthiirane and its oxirane analogue. *Biochemistry* **2009**, *48*, 9839–9847.
- (53) Tao, P.; Fisher, J. F.; Shi, Q.; Mobashery, S.; Schlegel, H. B. Matrix metalloproteinase 2 (MMP2) inhibition: DFT and QM/MM studies of the deprotonation-initialized ring-opening reaction of the sulfoxide analogue of SB-3CT. *J. Phys. Chem. B* **2010**, *114*, 1030–1037.
- (54) Zhou, J.; Tao, P.; Fisher, J. F.; Shi, Q.; Mobashery, S.; Schlegel, H. B. QM/MM studies of the matrix metalloproteinase 2 (MMP2) inhibition mechanism of (S)-SB-3CT and its oxirane analogue. *J. Chem. Theory Comput.* **2010**, *6*, 3580–3587.

Arylamide as potential selective inhibitor for matrix metalloproteinase 9 (MMP9) design, synthesis, biological evaluation, and molecular modeling

ORIGINALITY REPORT

19%

SIMILARITY INDEX

18%

INTERNET SOURCES

15%

PUBLICATIONS

7%

STUDENT PAPERS

PRIMARY SOURCES

1	Submitted to Universidade de Sao Paulo	3%
	Student Paper	

2	test.dovepress.com	2%
	Internet Source	

3	apb.tbzmed.ac.ir	2%
	Internet Source	

4	journals.plos.org	1%
	Internet Source	

5	jurnal.unpad.ac.id	1%
	Internet Source	

6	fjps.springeropen.com	1%
	Internet Source	

7	docsdrive.com	1%
	Internet Source	

8	biomed.nscc-gz.cn	1%
	Internet Source	

sipeg.univpancasila.ac.id

9	Internet Source	<1 %
10	Submitted to Monash University Student Paper	<1 %
11	Submitted to University of Malta Student Paper	<1 %
12	www.ejurnal-analiskesehatan.web.id Internet Source	<1 %
13	core.ac.uk Internet Source	<1 %
14	eprints.whiterose.ac.uk Internet Source	<1 %
15	Maywan Hariono, Pandu Hariyono, Rini Dwiastuti, Wahyuning Setyani, Muhammad Yusuf, Nurul Salin, Habibah Wahab. "Potential SARS-CoV-2 3CLpro Inhibitors from Chromene, Flavonoid and Hydroxamic Acid Compound based on FRET Assay, Docking and Pharmacophore Studies", Results in Chemistry, 2021 Publication	<1 %
16	doaj.org Internet Source	<1 %
17	Lung Wa Chung, W. M. C. Sameera, Romain Ramozzi, Alister J. Page et al. "The ONIOM	<1 %

Method and Its Applications", Chemical Reviews, 2015

Publication

18

www.freepatentsonline.com

Internet Source

<1 %

19

Florentinus D.O. Riswanto, Mira S.A. Rawa, Vikneswaran Murugaiyah, Nurul H. Salin et al. "Anti-Cholinesterase Activity of Chalcone Derivatives: Synthesis, In Vitro Assay and Molecular Docking Study", Medicinal Chemistry, 2021

Publication

<1 %

20

assets.researchsquare.com

Internet Source

<1 %

21

e-journal.usd.ac.id

Internet Source

<1 %

22

mdpi-res.com

Internet Source

<1 %

23

Pandu Hariyono, Rini Dwiastuti, Muhammad Yusuf, Nurul H. Salin, Maywan Hariono. "2-Phenoxyacetamide derivatives as SARS-CoV-2 main protease inhibitor: In silico studies", Results in Chemistry, 2022

Publication

<1 %

24

pubannotation.org

Internet Source

<1 %

25	rps.mui.ac.ir Internet Source	<1 %
26	www.scielo.br Internet Source	<1 %
27	Submitted to Western Illinois University Student Paper	<1 %
28	tel.archives-ouvertes.fr Internet Source	<1 %
29	www.spandidos-publications.com Internet Source	<1 %
30	Haines, Brandon E., C. Nicklaus Steussy, Cynthia V. Stauffacher, and Olaf Wiest. "Molecular Modeling of the Reaction Pathway and Hydride Transfer Reactions of HMG-CoA Reductase", Biochemistry, 2012. Publication	<1 %
31	mail.scialert.net Internet Source	<1 %
32	rupress.org Internet Source	<1 %
33	APB.tbzmed.ac.ir Internet Source	<1 %
34	Muchtaridi Muchtaridi, Muhammad Yusuf, Hasna Nur Syahidah, Anas Subarnas, Adel Zamri, Sharon Bryant, Thierry Langer. "	<1 %

Cytotoxicity Of Chalcone Of *Eugenia aquea*
Burm F. Leaves Against T47D Breast Cancer
Cell Lines And Its Prediction As An Estrogen
Receptor Antagonist Based On
Pharmacophore-Molecular Dynamics
Simulation

", Advances and Applications in Bioinformatics
and Chemistry, 2019

Publication

35	m.lookchem.com Internet Source	<1 %
36	www.cjcu.jlu.edu.cn Internet Source	<1 %
37	www.tandfonline.com Internet Source	<1 %
38	centaur.reading.ac.uk Internet Source	<1 %
39	hdl.handle.net Internet Source	<1 %
40	link.springer.com Internet Source	<1 %
41	theses.gla.ac.uk Internet Source	<1 %
42	Muhammad Yasin, Wardah Shahid, Muhammad Ashraf, Muhammad Saleem et al.	<1 %

" Targeting new N-furfurylated 4-chlorophenyl-1,2,4-triazolepropionamide hybrids as potential 15-lipoxygenase inhibitors supported with and studies ",
Journal of Biomolecular Structure and Dynamics, 2022

Publication

43

Nuti, Elisa, Anna Rita Cantelmo, Cristina Gallo et al. "N-O-Isopropyl Sulfonamido-Based Hydroxamates as Matrix Metalloproteinase Inhibitors: Hit Selection and in vivo Antiangiogenic Activity", Journal of Medicinal Chemistry

Publication

44

Pauline Zipfel, Christophe Rochais, Kévin Baranger, Santiago Rivera, Patrick Dallemagne. "Matrix Metalloproteinases as New Targets in Alzheimer's Disease: Opportunities and Challenges", Journal of Medicinal Chemistry, 2020

Publication

45

Rangasamy, Geronimo, Ortín, Coderch, Zapico, Ramos, de Pascual-Teresa. "Molecular Imaging Probes Based on Matrix Metalloproteinase Inhibitors (MMPIs)", Molecules, 2019

Publication

<1 %

<1 %

<1 %

46	Role of Proteases in Cellular Dysfunction, 2014. Publication	<1 %
47	Scholar.sun.ac.za Internet Source	<1 %
48	Univendspace.univen.ac.za Internet Source	<1 %
49	doi.org Internet Source	<1 %
50	eprints.ucm.es Internet Source	<1 %
51	portlandpress.com Internet Source	<1 %
52	www.future-science.com Internet Source	<1 %
53	www.jbc.org Internet Source	<1 %

Exclude quotes On
Exclude bibliography On

Exclude matches < 5 words